P. Lalande
(Onera)
V. Mazur
(National Severe Storms Laboratory)

E-mail: philippe.lalande@onera.fr

A Physical Model of Branching in Upward Leaders

The physical processes leading to branching and physical factors affecting branching features are poorly understood. We are applying the tested physical model of axisymmetrical leader development following the streamer-leader transition to a 3-dimensional propagation of the leader with branching. The propagation of the leader is driven by the potential drop at the leader tip. The branching occurs when the drop potential at the leader tip reaches a threshold. The space charge around the leaders self regulates the total number of active branches by reducing the available potential for the propagation. The model has been applied to simulate the time evolution of an upward leader started from a tall ground structure and developing in an electric field produced by a mature thunderstorm. We are satisfied with the fact that the results of computer simulation of branching leader closely resemble branching of upward positive leaders triggered by tall structures depicted in high-speed video images.

Introduction

The physical processes that lead to branching, and the physical factors that affect branching features remain among several unresolved issues in our understanding of lightning development. The questions, such as: Under what conditions does the leader start branching? How does the branching form? And how do the neighboring branches interact, and does this interaction lead to the arrest of the propagation of some branches, while others continue to propagate? All these questions come to the mind of an observer who views and analyzes the fascinating high-speed video images of branched leaders.

Some laboratory experiments and field observations have exposed features of branching processes. For example, we know, from studies of discharges developing within a layer charge inserted in plastics [1] that branching channels prefer space charge regions and avoid regions that are free of space charge. A similar conclusion can be drawn from the analysis of maps of lightning radiation sources, obtained with the time-of-arrival technique, that have their highest density within the charge layers of a thundercloud.

Computer models of lightning development that considered induced charges on a leader channel have produced only single, vertical channels of intracloud and negative cloud-to-ground flashes [2], [3]. Lightning branching was introduced in the numerical models of a thunderstorm based on the stochastic dielectric breakdown concept [4], [5]. These fractal models, although applying the equipotential hypothesis by Kasemir [6] to floating leaders, simulated macroscopic behavior of leaders without addressing the internal physical processes involved in leader development. Also, a large space resolution of storm models cannot reproduce the actual sizes of leader cross-sections and the dimensions of leader branching.

The objective of this study is to address the processes of branching first for a unidirectional positive leader, as a less complex type of leader development. We are applying the tested physical model of axisymmetrical leader development following streamer-leader transition to a 3-dimensional propagation of a leader with branching. In the course of creation of the model of a branched leader we define the model's variables and range of those variables that could be confirmed by field observations or measurements. For the computer simulation of the branching leader, we used a simplified model of thunderstorm charges, in order to determine the sensitivity of the branching model to various parameters of the model.

Principles of modeling a straight-propagating upward leader

In modeling the propagation of upward leaders, we applied the principles used in modeling the development of a straight leader, as a non-time-dependent extension of the already-existing leader channel by the streamer-leader transition process, regardless of the mechanism of leader initiation [7]. During the streamer-leader transition, cold streamers, which fan like a cone ahead of the leader tip, produce, in the course of leader extension, a space charge in the form of a cylindrically shaped envelope surrounding the hot plasma channel of the leader. This space charge is stationary, and remains so for a period of time much longer than the lifetime of a lightning flash.

The variables that describe the electrical conditions governing development of the leader, some of which are a function of an altitude, z, are:

- $U_{atm}(z)$ - ambient potential, assumed to be distributed linearly.
- $U_{extr}(z)$ - potential at the leader tip.
- $U_{ce}(z)$ - potential produced by a space charge of corona streamers.
- ΔU_T - potential difference ahead of the tip of the leader, also called "potential drop".
- E_0 - ambient electric field, constant for linear potential distribution.
- E_{int} - internal electric field in a leader channel due to its finite resistivity.
- E_{stab} - stability field, which is an electric field inside the streamer zone, assumed to be 400 kV m^{-1} and 800 kV m^{-1}, for positive [8][9][10] and negative streamers [11], respectively.
- q_{ce} – space charge per unit length generated by the streamer-leader transition (C m^{-1}).

The variables that describe the physical dimensions of the leader are:

- H - height of the structure, from which leader is initiated.
- L - length of the developing leader.
- L_C - length of the streamer zone ahead of the leader.
- a_{ce} - a radius of a space charge envelope surrounding the leader.

The variables that describe the atmospheric conditions along the leader path, and a function of altitude, z, are:

- $P(z)$ - ambient pressure, P_0 is the atmospheric pressure at the ground level.
- $T(z)$ - ambient temperature, T_0=300 K is a normal temperature.
- $\rho(z)$ - air density, $\rho(z) = [P(z)\ T_0] / [P_0\ T(z)]$.

The potential distribution along and immediately ahead of the developing leader is depicted in figure 1. This potential distribution is affected by the presence of the space charge envelope. The magenta line indicates the potential distribution due to the ambient field E_o. The tall structure, from which leader initiates is assumed to be a perfect conductor, and thus on a zero ground potential. The leader is resistive, so its current produces a potential gradient of E_{int}, assumed to be constant. The space charge region ahead of the leader affects longitudinal propagation of the leader, by reducing the electric field at the leader tip. The dotted curve ahead of the leader tip depicts the variation of the potential distribution from the leader tip to the ambient electric field. The potential difference available to sustain the leader propagation is the potential drop ΔU_T at the leader tip, and is expressed by equations 1- 4:

$$\Delta U_T = U_{extr}(H+L) - \left[U_{atm}(H+L) + U_{ce}(H+L)\right] \tag{1}$$

where

$$U_{atm}(H+L) = -E_o(H+L) \tag{2}$$

$$U_{extr}(H+L) = -E_{\text{int}} L \tag{3}$$

$$U_{ce}(H+L) = U_{ce1}(H+L) + U_{ce2}(H+L) \tag{4}$$

U_{ce1} is the potential on the axis due to the space charge, and U_{ce2} is the component due to the image on the ground.

In our simplified model, the space charge is in form of a cylinder of radius ace and of length $L+L_c$, with a uniform charge of linear density q_{ce} and a total charge of $q_{ce}L$. With these assumptions, the two components of the potential due to the space charge have the following expression:

$$U_{ce1} = \frac{q_{ce}L}{4\pi\varepsilon_o a_{ce}^2 (L+L_c)} \times \left[-\left(L^2 + L_c^2\right) + a_{ce}^2 \ln\left[\frac{\sqrt{a_{ce}^2 + L_c^2} + L_c}{\sqrt{a_{ce}^2 + L^2} - L}\right] + L\sqrt{a_{ce}^2 + L^2} + L_c\sqrt{a_{ce}^2 + L_c^2} \right] \tag{5}$$

$$U_{ce2} = -\frac{q_{ce}L}{4\pi\varepsilon_o a_{ce}^2 (L+L_c)} \times \left[(2H+L)^2 - (2H+2L+L_c)^2 + a_{ce}^2 \ln\left[\frac{\sqrt{a_{ce}^2 + (2H+L)^2} - (2H+L)}{\sqrt{a_{ce}^2 + (2H+2L+L_c)^2} - (2H+2L+L_c)}\right] + (2H+2L+L_c)\sqrt{a_{ce}^2 + (2H+2L+L_c)^2} - (2H+L)\sqrt{a_{ce}^2 + (2H+L)^2} \right] \tag{6}$$

The linear charge density of ~50 μC m^{-1} and ~145 μC m^{-1} for a positive and a negative leader, respectively, were derived from laboratory measurements [12][13]. Lalande et al. [7] assumed the value of the radius a_{ce} of the space charge envelope as 0.5 m for leaders of both polarities. In a simplified and consistent physical model [7][12], this value fits the measurements of Willet et al. [14] for a case of a rocket-triggered lightning. The corona length L_c is inferred from the stability field E_{stab} and ΔU_T by the (7):

$$L_c = \frac{\Delta U_T}{E_{STAB}} \tag{7}$$

Electrical discharges are sensitive to air density variation, such as described by Paschen's Law. Lalande [15] shows that, for lightning leaders, the ambient field $E_o(z)$ has to be corrected by the factor , $1/\rho(z)$ in order to take into account the air density variation with altitude.

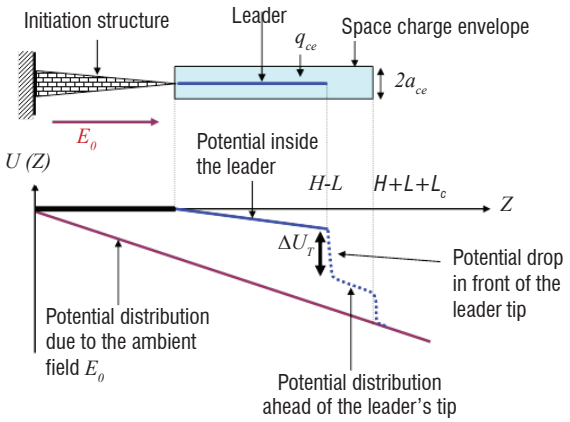

Figure 1 - Longitudinal potential distribution along the path of an upward positive leader developing from a ground structure

Modeling the 3-D propagation of the straight leader in a thunderstorm

For computer simulation of the 3-D leader propagation, we used the electrostatic model of a mature storm [3]. This storm model is represented by four charged cylinders with a constant charge density (figure 2). The vertical potential profile from ground to 1500 m altitude, computed for this model, is in close agreement with the potential profile measured by Willet et al [14] during a rocket-triggered lightning experiment.

Figure 3 depicts the concept of 3-D propagation of a leader segment that is assumed in our model. A new direction of propagation of the leader tip is chosen at each time step, and a new segment of the leader and its associated space charge is added to the preceding segment. In adaptation of the axisymetrical model of the leader to the 3-D development, we replaced the space charge envelopes of the leader segments with the sets of equivalent charge lines. Their effects on the electrical potential are similar to those produced by the space charge envelopes. We use the Boundary Element Method (BEM) that is based on the solving of integral equations to compute the new electrostatic setup and the resulting voltage drop at the leader tip at each time step.

The direction $\overrightarrow{d_{max}}$ is towards the maximum potential drop, which is computed at a distance $2L_C$ from the tip on a sphere centered at the

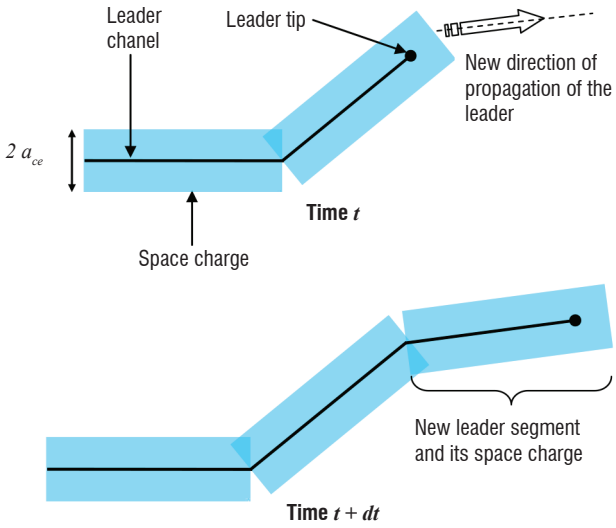

Figure 3 - Depiction of the 3-D propagation of a leader filament in time steps

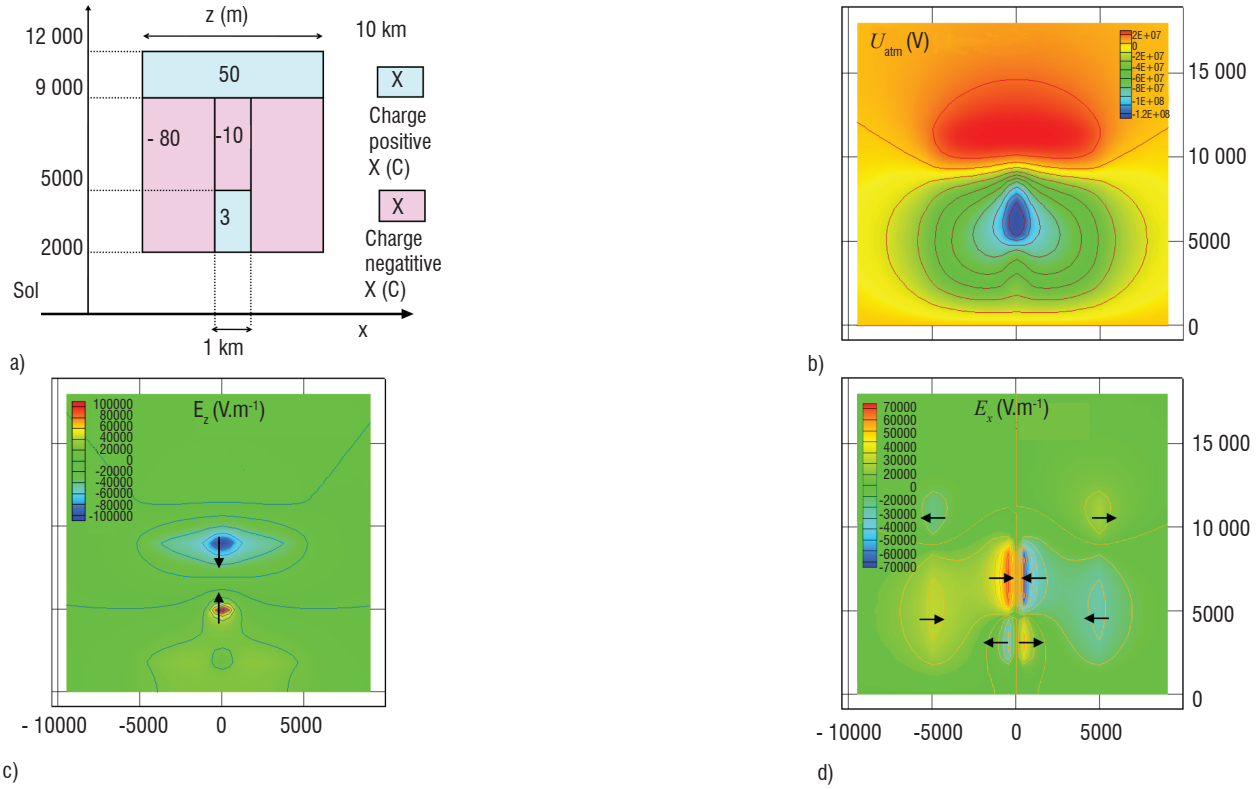

Figure 2 - Vertical slides *(x, y=0, z)* of (a) electric charge distribution inside a mature thundercloud [3], (b) atmospheric potential UATM, (c) vertical component of the atmospheric field *Ez*. and (d) horizontal component of the atmospheric field *Ex*. The black arrows show the direction where the *E*-field intensifies.

leader tip. The computation is not performed at L_c where the effects of both leader and space charge are maximal, but slightly ahead of it, to make it more sensitive to the cloud potential. In choosing the direction of propagation the model takes into account the stochastic character of leader's motion. We assume that the final direction $\vec{d}$ of leader propagation for the angle θ is determined by a Gaussian distribution centered on 0°, with a standard deviation of 45°, and for the angle φ by uniform distribution from 0 to 360° (figure 4).

Leader branching criterion

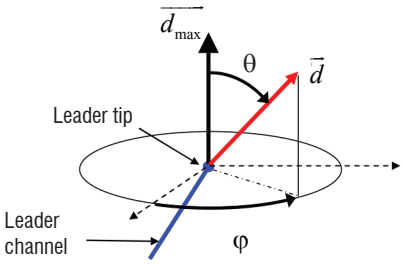

Figure 4 - Choosing the direction of leader propagation $\vec{d}$ at each time step (angles θ, φ). $\vec{d}_{max}$ is the direction where the potential drop between the leader tip and a point at $2L_c$ ahead of the leader is at its maximum.

The most challenging task in modeling branching leaders is to determine the electrostatic criteria for branching. Here is what we learned from studying upward positive leaders starting from tall towers [16]: single-channel upward leaders are triggered either by (1) passing-by negative leaders of intracloud flashes, or (2) by return strokes of positive CG flashes. In the first case, these upward leaders start branching when they approach the cloud base above. It is known that the potential drop ahead of the ascending upward leader is greater near the cloud base than at the ground level. In the second case, the upward leaders branching occurs right from the start (the top of the tall structure), triggered by return strokes of nearby positive CG flashes. Our explanation of the noticed difference in when and where the leader branching starts is as follows: The impact of the electric field change produced by return strokes of $+CG$ flash on the triggering of an upward leader is much greater than that of the intracloud negative leader passing by, due to its much higher current and speed. We interpret the high-speed video observations of branching in positive upward leaders from tall towers referred to here as indicating that branching occurs at rather high electric field changes, and therefore, at the potential drops values that are greater than those needed for development of a single, non-branched leader channel.

We also recognize that branching of the leader may affect the speed of leader propagation, in comparison with that of a non-branching leader, and make such assumption in our model. An empirical formula (8) expresses the relationship between the leader's velocity and the potential drop ahead of the leader ΔU_T, which is the driving force of the leader progression, in relationship to the variable ΔU_B that represents the potential drop required to start branching.

$$V_L = V_{LR\max}\left(1 - e^{\frac{-2|\Delta U_T|}{\Delta U_B}}\right) \quad (8)$$

The variation of the leader's velocity as a function of the potential drop ΔU_T, with ΔU_B being constant, is depicted in figure 5 for different values of V_{LRmax} and ΔU_B.

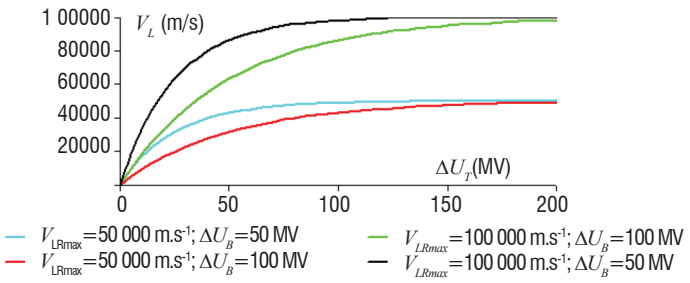

Figure 5 - Evolution of the leader velocity as a function of the potential drop at the leader tip ΔU_T for different values of V_{LRmax} and ΔU_B.

The dynamics of branching for a natural upward leader is seen in figure 6a, for an upward positive leader started from a tall tower. In this example and in numerous others obtained with a high-speed video system, the characteristic feature of branching is the splitting of a single channel into two branches [13]. There is also indication of a prevalent angle between two new branches, the value of which is hard to obtain from the two-dimensional images. In our model, branching also always occurs as the splitting of a single channel into two, after ΔU_T reaches or exceeds ΔU_B (figure 6b). After that, each part of the branch develops as a single channel, with its own velocity, and the possibility of further branching, depending upon the potential drop ΔU_T at its tip .

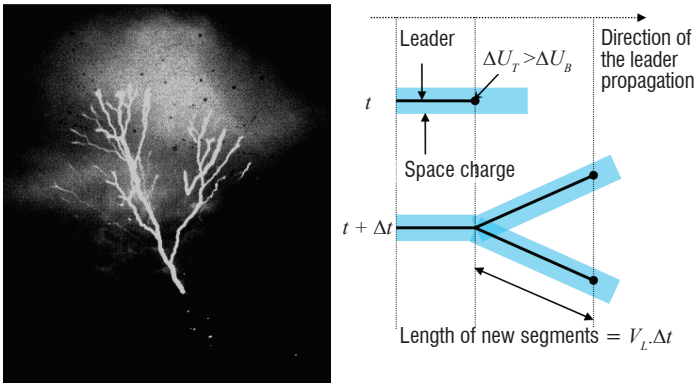

Figure 6 - (a) Composite image of an upward branching leader (courtesy of Tom Warner) and (b) depiction of the branching concept model.

The range of values of the branching criterion ΔU_B is determined from the comparison of 3-dimensional lightning mapping observations, obtained with the Lightning Mapping Array (LMA), with the electric potential profile inferred from balloon soundings of the electric fields in New Mexico mountain thunderstorms [17]. The altitude histogram of the flash radiation sources in figure 7 shows two maxima of radiation source density: at the band of 6 - 7 km, and at the band of 9 - 11 km. These are two bands where leaders propagate horizontally and also branch within. Negative leaders produce much stronger VHF radiation than positive ones. This strong radiation identifies the altitudes of 9-11 km as associated with a negative leader development zone and the altitudes of 6-7 km as associated with positive leader propagations. The bidirectional leader originates at the altitude of ~8 km, and propagates vertically until its upper and lower tips reach 9 and 7 km altitudes, respectively. During its vertical development phase, the leader is in electrostatic equilibrium with the ambient potential

profile (marked by the blue line in figure 7). Assuming that the positive leader starts branching only after reaching the 6 -7 km band, we infer, from the potential profile in figure 7, the corresponding values of the branching potential drop ΔU_B to be in the range of 20 to 50 MV. Adjusted for the air density at these altitudes, the values for ΔU_B at mean sea level would be from 35 MV to 105 MV.

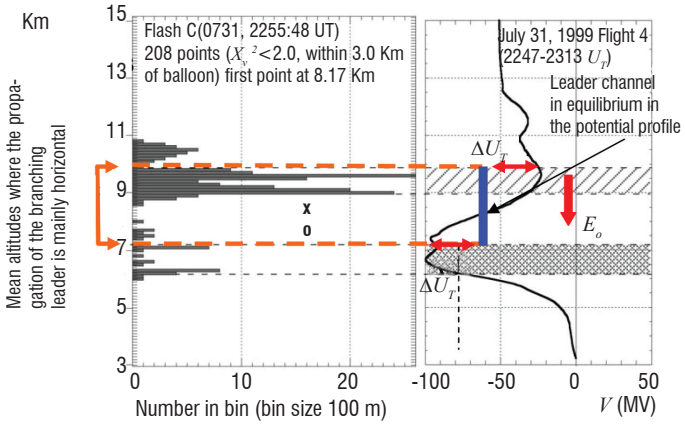

Figure 7 - (a) Altitude histogram of lightning radiation sources. The cross marks the altitude of the first LMA source and the likely location of flash initiation. (b) The vertical potential profile inferred from balloon soundings of the electric field in New Mexico mountain thunderstorms. The circle indicates the altitude of the balloon at the time of the flash [17].

The dotted lines and cross-hatching in the histogram identify the boundaries of the regions with most radiation sources. The upper region is associated with negative polarity leaders and the lower region with positive polarity leaders. The blue vertical line corresponds to the potential of the vertical part of the bidirectional leader channel before it propagates horizontally and branches. The red horizontal bidirectional arrows correspond to the potential drop available at each extremity of the bidirectional leader before the branching process occurs.

Computer simulation of branching in upward leader

Computer simulation of branching was performed for an upward positive leader that started from a tall grounded structure during a mature thunderstorm (see model in figure 2), the vertical potential profile of which is presented in figure 2b. In a thunderstorm with this ambient potential profile, the leader can propagate to a maximum altitude that is slightly below 10 km. However, when conditions for branching exist, the duration of a time step affects the computer simulation of the branching structure. Without branching, there is no influence of the time step on the results of simulation.

With the drop potential ΔU_T equal to or above the branching criteria ΔU_B, the leader splits into two branches. The distance d_{bb} between the two new segments, measured horizontally between tips of branches, depends on the time step, as shown in the following expression:

$$d_{bb} = 2V_L \Delta t \sin\alpha \qquad (9)$$

where α is the angle between the two new segments with a mean value of 45°. The smaller the time step, the smaller the distance d_{bb}. The number of active leader tips (N_{al}) increases following the mathematical law $N_{al} = 2^{\frac{t}{\Delta t}}$, where t is the period of time since the first branching occurs.

When there is no physical limitation in the branching process, the branching structure calculated for three time steps (Δt=0.5 ms, Δt=1 ms, Δt=2 ms) is as shown in figure 9.

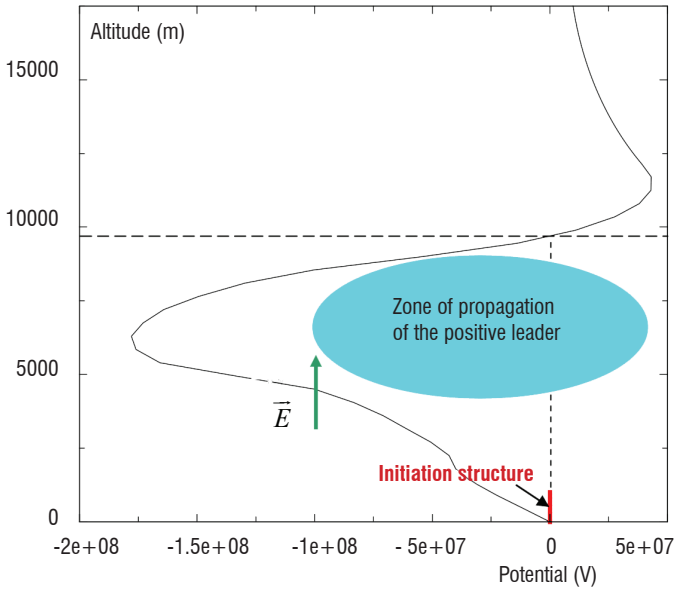

Figure 8 - Vertical ambient potential profile of the mature thunderstorm structure shown in figure 2. The vertical red bar identifies the tall structure from which a positive upward leader develops. The horizontal dashed line indicates the maximum altitude for the positive leader propagation.

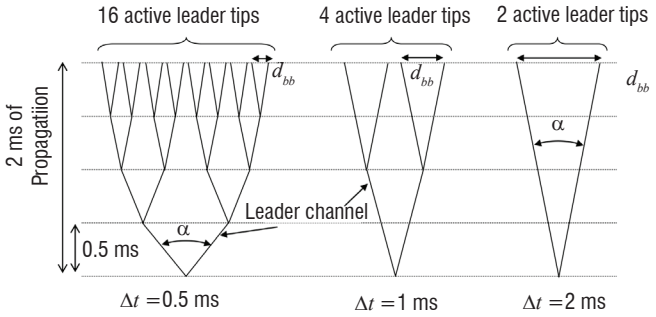

Figure 9 - Depiction of the unrestricted development of branches for three time steps (Δt=0.5 ms, Δt=1 ms, Δt=2 ms) for a 2 ms-long propagation. In this conceptual figure, and also in figure 10, the angle α between branches in all figures is the same, and is shown as different for the illustration purpose only.

In our model, the distance between branches plays a significant role in the leader propagation because of the presence of a space charge envelope of the same polarity on each branch. The drop potential of a neighboring branch may be drastically reduced by the close proximity of the space charge envelope, which may arrest the development of a new branch. The smaller this distance, the greater the screening effects of the space charge of one branch on the potential drop ΔU_T of the other branch. When two new branches are created at each time step, and the distance between the two new leader tips is big enough, both branches can propagate; otherwise one of them stops. In the example shown in figure 10, only two active leader tips remain at the end of 2 ms-long propagation, regardless of the choice of time step. It is also apparent that the larger the space charge per unit length (q_{ce}), the smaller the number of branches produced. Thus, the electrostatic interaction between leader's parts limits the development of new branches in our model.

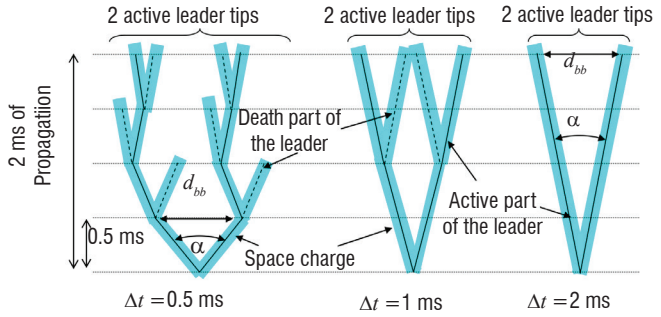

Figure 10 - Depiction of the development of a branching upward leader as a function of the time step when the effect of space charge envelopes is considered. The blue zone identifies the space charge envelope of the branch. The full line is associated with an active part of the leader channel. The dashed line is a branch, which stopped propagating. d_{bb} is the distance between the two new leader tips.

We calculate the branching characteristics of an upward leader with the space charge-per-unit length (q_{ce}) of 100 μCm^{-1}, which develops with time steps of Δt=0.5 ms, Δt=1 ms, and Δt=2 ms (figure 11). The branching criterion ΔU_B is set at 30 MV. The mean vertical velocity of the branched leader is 6.4 x 10^4 m s^{-1}. The final altitude reached by the branched leader is 8000 m, which is 2000 m lower than the maximum theoretical altitude shown in figure 8. As seen in the plot in figure 11a, there is a weak dependency of the final altitude on the duration of the time step. Figure11b shows the time evolution of the total number of branches, as well as of the total number of arrested branches. The difference between these two numbers gives the number of active branches. Both the number of branches and the number of arrested branches depend on the duration of the time step. As figure 11b shows, these two numbers are not so different.

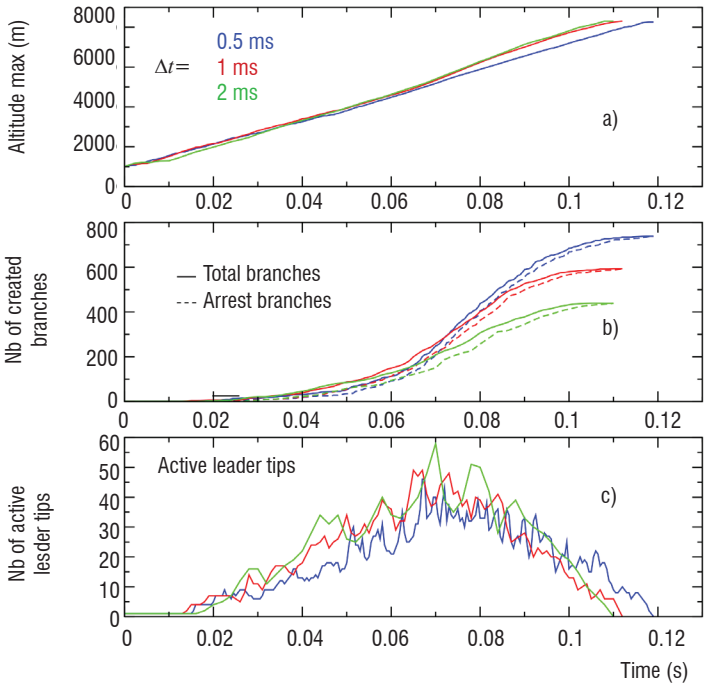

Figure 11 - Effect of the time step duration Δt on branching characteristics of upward leader. (a) Maximal vertical extension of the upward leader. (b) The total number of branches created at a given time and the total number of arrest branches. (c) The total number of active branches. Parameters of computation ΔU_B = 30 MV, q_{CE} = 100 μC m^{-1}, Δt=0.5 ms, 1 ms and 2 ms.

The figure 11c depicts the number of active leader tips as a function of time. The branching starts at altitude of 2000 m. The number of active leader tips increases up to an altitude of 5000 m where the maximum potential values are found, and then decreases at higher altitudes. It is clearly seen in figure 11c that the number of active leader tips is mostly independent of the time step duration. The upward leader propagates longer than 100 ms before it stops, which is within the range of durations commonly observed in nature for upward positive leaders.

For the same three values of the time step duration, we have plotted all leader branches created at the end of the upward leader propagation (figure 12). The results show that the total horizontal extension of the discharge is larger for larger time steps. This is due to a few branches that have a mostly horizontal propagation during a few steps and then stop, while the majority of active branches continue their propagation in the region of high ambient potential. At the end of the propagation, the zones where the majority of branches are located are quite similar and independent of the time step duration.

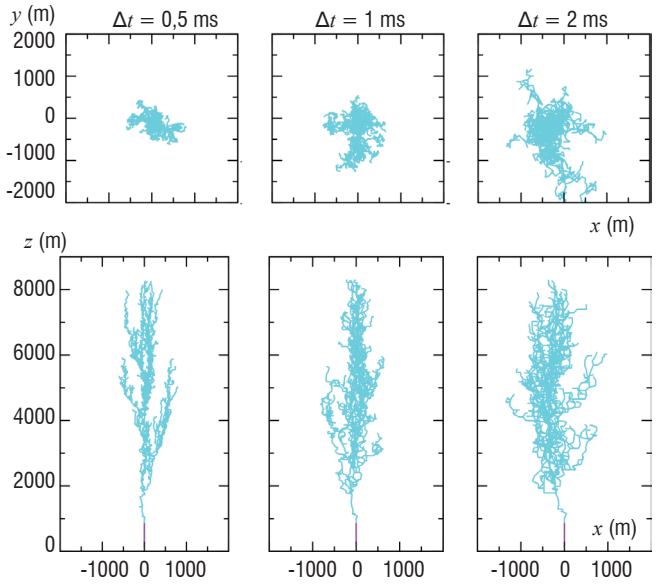

Figure 12 - Effect of the time step on the total leader branches at the end of the discharge propagation. q_{ce}=100 μC m^{-1} et ΔU_B=30 MV.

Conclusion

The modeling of the three-dimensional propagation of a branching leader has been based on an electrostatic model, the parameters of which have been inferred from physical models and validated by observations. The propagation of the leader is driven by the potential drop at the leader tip, which differs from most previous fractal models of branching that used the electric field as a propagation criterion. Branching, by splitting a branch into two new branches, occurs when the drop potential at the leader tip reaches a threshold, which we inferred from LMA observations and the ambient electric field measurements in a thunderstorm. In the model, the space charge around the leaders regulates the total number of active branches by reducing the available potential for their propagation. The model has been applied to simulate the time evolution of an upward leader developing from the tall ground structure. We are satisfied with the fact that the results of computer simulation of a branching leader resemble the branching structures in high-speed video images of upward positive leaders triggered by tall structures. One may expect the results of branching simulation to differ for different storm stages, and thus, the different potential profiles ■

Acknowledgements

The authors wish to thank Isabelle L'Helgoualc'h for her major contribution to this work.

References

[1] E. R. WILLIAMS, C. M. COOKE, ET K. A. WRIGHT - *Electrical Discharge Propagation in and Around Space Charge Clouds*. Journal of Geophysical Research, vol. 90, n°. D4, pp. 6059-6070, 1985
[2] R. SOLOMON, M. BAKER - *A One-Dimensional Lightning Parameterization.* Journal of Geophysical Research, vol. 101, n °. D10, pp. 14,983-14,990, June 1996
[3] V. MAZUR et L. H. RUHNKE - *Model of Electric Charges in Thunderstorms and Associated Lightning*. Journal of Geophysical Research, vol. 103, n°. D18, pp. 23,299-23,308, 1998
[4] E. R. MANSELL, D. R. MACGORMAN, C. L. ZIEGLER, J. M. STRAKA - *Simulated Three-Dimensional Branched Lightning in a Numerical Thunderstorm Model*. J. Geophys. Res., vol. 107, pp. 12, May 2002
[5] J. A. RIOUSSET, V. P. PASKO, P. R. KREHBIEL, R. J. THOMAS, W. RISON - *Three-Dimensional Fractal Modeling of Intracloud Lightning Discharge in a New Mexico Thunderstorm and Comparison with Lightning Mapping Observations*. Journal of Geophysical Research, vol. 112, n°. D15, August 2007
[6] H. W. KASEMIR - *A Contribution to the Electrostatic Theory of a Lightning Discharge*. Journal of Geophysical Research, vol. 65, n°. 7, pp. 1873-1878, 1960
[7] P. LALANDE, A. BONDIOU-CLERGERIE, G. BACCHIEGA, I. GALLIMBERTI - *Observations and Modeling of Lightning Leaders*. Comptes Rendus Physique, vol. 3, n°. 10, pp. 1375-1392, December 2002.
[8] C. T. PHELPS - *Field-Enhanced Propagation of Corona Streamers*. Journal of Geophysical Research, vol. 76, n°. 24, pp. 5799-5806, 1971
[9] R. F. GRIFFITHS, C. T. PHELPS - *The Effects of Air Pressure and Water Vapour Content on the Propagation of Positive Corona Streamers, and Their Implications to Lightning Initiation*. Quarterly Journal of the Royal Meteorological Society, vol. 102, n°. 432, pp. 419-426, April 1976
[10] R. F. GRIFFITHS, C. T. PHELPS - *Positive Streamer System Intensification and its Possible Role in Lightning Initiation*. Journal of Atmospheric and Terrestrial Physics, vol. 36, n°. 1, pp. 103-111, january 1974.
[11] Groupe des Renardières - *Negative Discharges in Long Air Gaps at Les Renardières, 1978 Results*. ELECTRA, 1981
[12] A. BONDIOU, I. GALLIMBERTI - *Theoretical Modelling of the Development of the Positive Spark in Long Gaps*. Journal of Physics D: Applied Physics, vol. 27, n°. 6, pp. 1252-1266, june 1994
[13] I. GALLIMBERTI, G. BACCHIEGA, A. BONDIOU-CLERGERIE, P. LALANDE - *Fundamental Processes in Long Air Gap Discharges*. Comptes Rendus Physique, vol. 3, n°. 10, pp. 1335-1359, December 2002
[14] J. WILLETT, D. DAVIS, P. LAROCHE - *An Experimental Study of Positive Leaders Initiating Rocket-Triggered Lightning*. Atmospheric Research, vol. 51, n°. 3-4, pp. 189-219, July 1999
[15] P. LALANDE - *Etude des conditions de foudroiement d'une structure au sol*. Université Paris XI Orsay, 1996. Ph. D. Thesis.
[16] T. WARNER - *Personal Communication*
[17] L. M. COLEMAN, T. C. MARSHALL, M. STOLZENBURG, T. HAMLIN, P. R. KREHBIEL, W. RISON, R. J. THOMAS - *Effects of Charge and Electrostatic Potential on Lightning Propagation*. J. Geophys. Res., vol. 108, pp. 27 , May 2003

Acronyms

BEM (Boundary Element Method)
LMA (Lightning Mapping Array)

AUTHORS

Philippe Lalande graduated from the "Ecole Supérieure de Physique Chimie de Paris" Paris (1992) and received a PhD degree in Plasma Physics from University Paris XI (1996). He joined Onera in 1996 where he has been involved both in the modelling of lightning interaction with aircraft and in the development of onboard atmospheric sensors. He is the head of the lightning and plasmas Research Unit at Onera Chatillon.

Vladislas Mazur was educated in Russia, and emigrated to the United States in 1978. He received his Ph.D. in Electrical Engineering from the University of Oklahoma, in 1981. He has worked at the National Severe Storms Laboratory in Norman, Oklahoma, since 1984 as a Physicist. He has a long history of scientific collaboration with scientists at Onera in lightning–aircraft interaction studies, and his main interests are physics of lightning processes and its application to lightning protection.